Supplementary Information

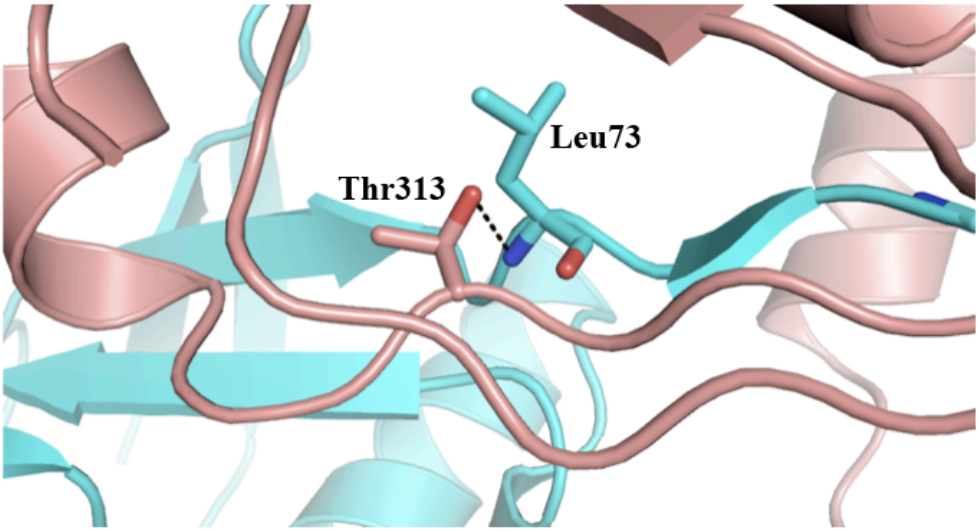

Fig. S1. Representation of the MIC-CAP-associated mutation. Model of the potential interaction that Thr313 adopts in the model of AMSH bound to Lys63-diubiquitin. AMSH is shown in pink ribbon, the distal ubiquitin of Lys63-diubiquitin is shown in cyan ribbon. Black dashes indicate the potential hydrogen-bonding interaction between Thr313 of AMSH and the backbone amine of Leu73 of the distal ubiquitin.

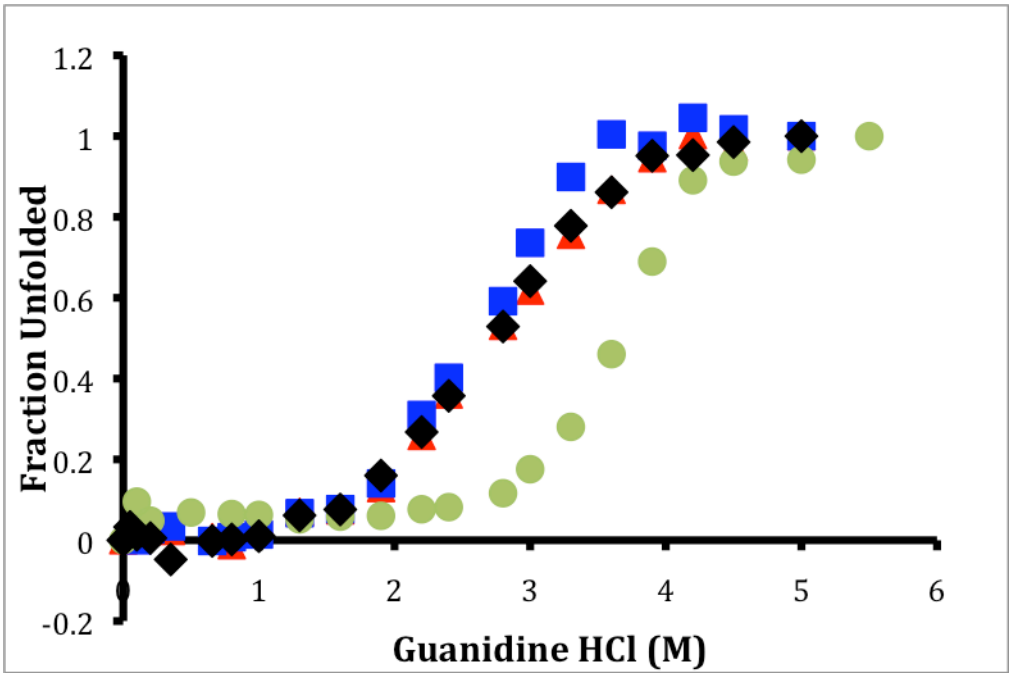

Fig. S2. Fraction unfolded curves comparing the thermodynamic stability of AMSH244WT (diamonds), AMSH219WT (squares), AMSH219T313I (triangles), and AMSH-LP DUB domain (circles) assessed by increasing concentrations of GdHCl monitored by CD spectroscopy at 220 nm. The fraction unfolded curves of AMSH244WT and AMSH-LP DUB domain were reported previously (Davies, C.W. *et al. J Mol Biol* (2011)).

Supplementary Table 1. Stability Data

Protein	ΔG_{H2O} (kcal.mol^{-1})	$[GdHCl]_{0.5}$ (M)	m (kcal.mol^{-1}.M^{-1})
AMSH244WT*	3.7	2.7	-1.4
AMSH219WT	3.6	2.5	-1.4
AMSHT313I	2.9	2.7	-1.1
AMSH-LP DUB*	4.9	3.5	-1.4

*Data reported in our previous paper (Davies, C.W. *et al. J Mol Biol* 2011)

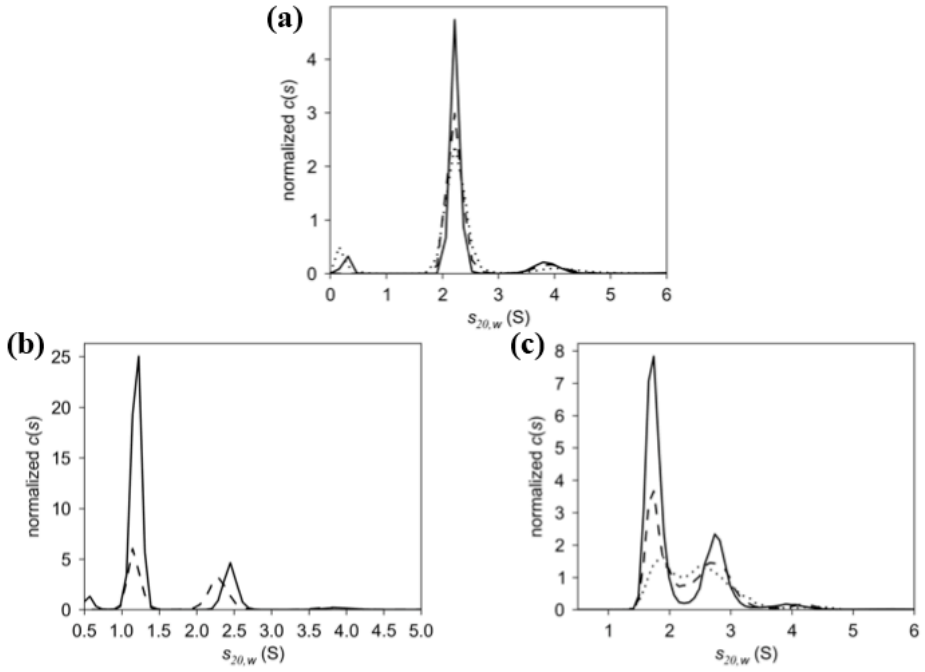

Fig. S3. c(s) distributions of (a) AMSH219, (b) AMSH:ubiquitin, and (c) AMSH:Lys63-diubiquitin. Three concentration series were used for AMSH219 and AMSH:Lys63-diubiquitin, while two concentrations were used for AMSH:ubiquitin. It was found that AMSH219 sediments at 2.2S, AMSH:ubiquitin complex at 2.4S, and AMSH:Lys63-diubiquitin at 2.8S, with excess ubiquitin and diubiquitin at 1.2S and 1.7S respectively. Plots were normalized to the peak area of AMSH219 or the peak area of the complexes.

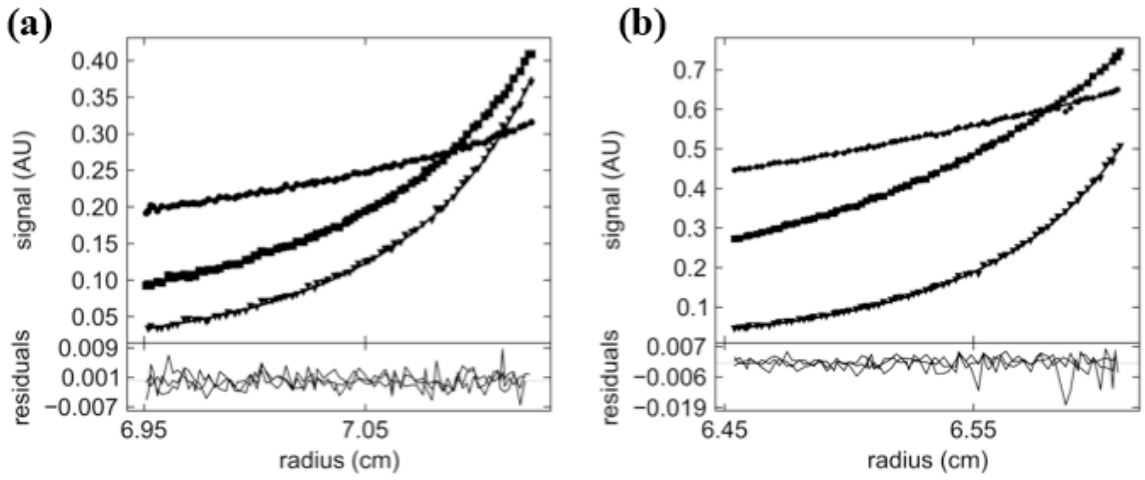

Fig. S4. Representative sedimentation equilibrium profiles for (a) AMSH:ubiquitin and (b) AMSH:Lys63-diubiquitin to determine the molecular weights of the complexes.

Supplementary Table 2. AUC Data

Protein	**$S_{20,w}$ (S)**	**v-bar ($ml.g^{-1}$)**	**Theoretical molecular weight (Da)**	**Calculated molecular weight (Da)**
AMSH219	2.2	0.7338	23120	22000 [SV]
AMSH-SH3	1.3, 2.5	0.7187	7561 / 30664	8600 / 23000 [SV]
AMSH-UIM-SH3	1.3, 2.6	0.7170	12588 / 35690	12000 / 34000 [SV]
AMSH-Ub	1.2, 2.4	0.7247	8976 / 32079	8000 / 24000 [SV] 8900 ± 2900 / 31500 ± 12000 [SE]
AMSH-DiUb	1.7, 2.8	0.7293	17935 / 41037	17000 / 34000 [SV] 14700 ± 3700 / 44000 ± 10000 [SE]

SV-Sedimentation velocity
SE-Sedimentation equilibrium

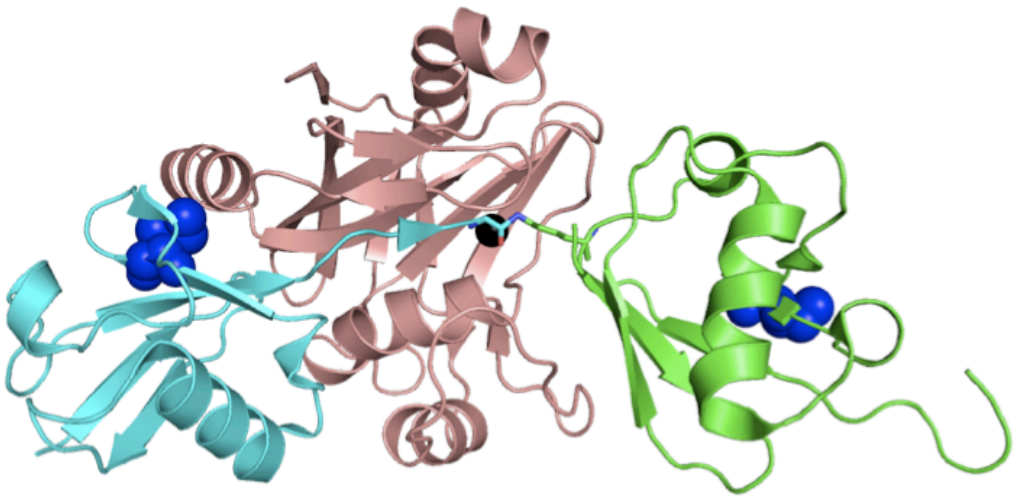

Fig. S5. Model of AMSH bound to Lys63-diubiquitin. Representation of AMSH (pink ribbon) bound to a Lys63-linked diubiquitin, showing Ile44 as blue spheres in both the proximal (green ribbon) and distal (cyan ribbon) ubiquitins. The active-site Zn^{2+} is shown as a black sphere.

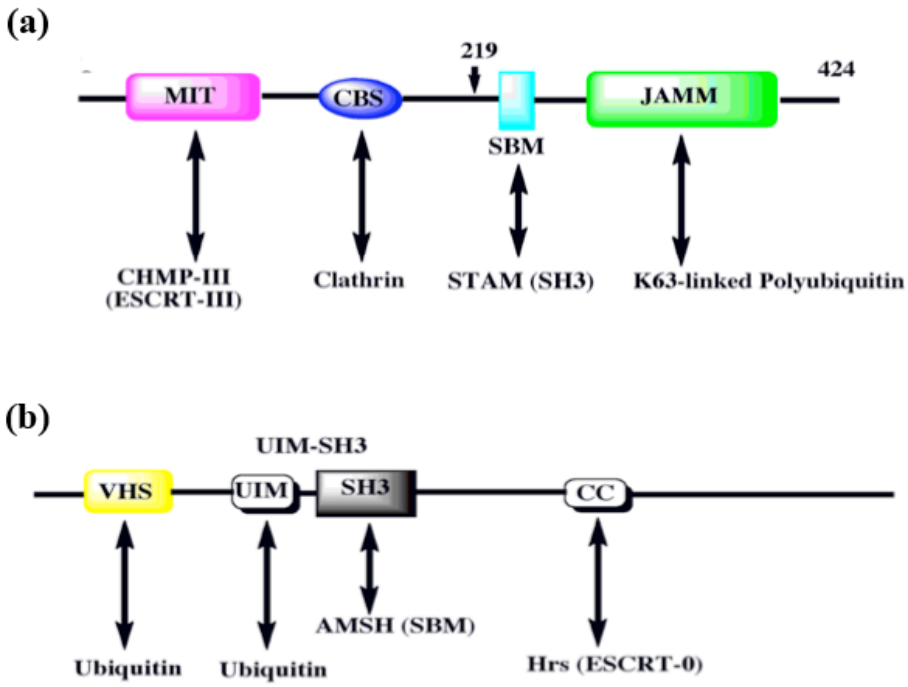

Fig. S6. Domain diagram of (a) full-length AMSH and (b) full-length STAM indicating the appropriate binding partners associated with each domain. Abbreviations are as follows: MIT (microtubule interacting and transport), CBS (clathrin binding sequence), SBM (SH3-binding motif), JAMM (JAB1/MPN/MOV34), VHS (Vps27, Hrs, STAM), UIM (ubiquitin-interacting motif), SH3 (Src homology 3 domain), Hrs (hepatocyte growth factor (HGF)-regulated tyrosine kinase substrate).

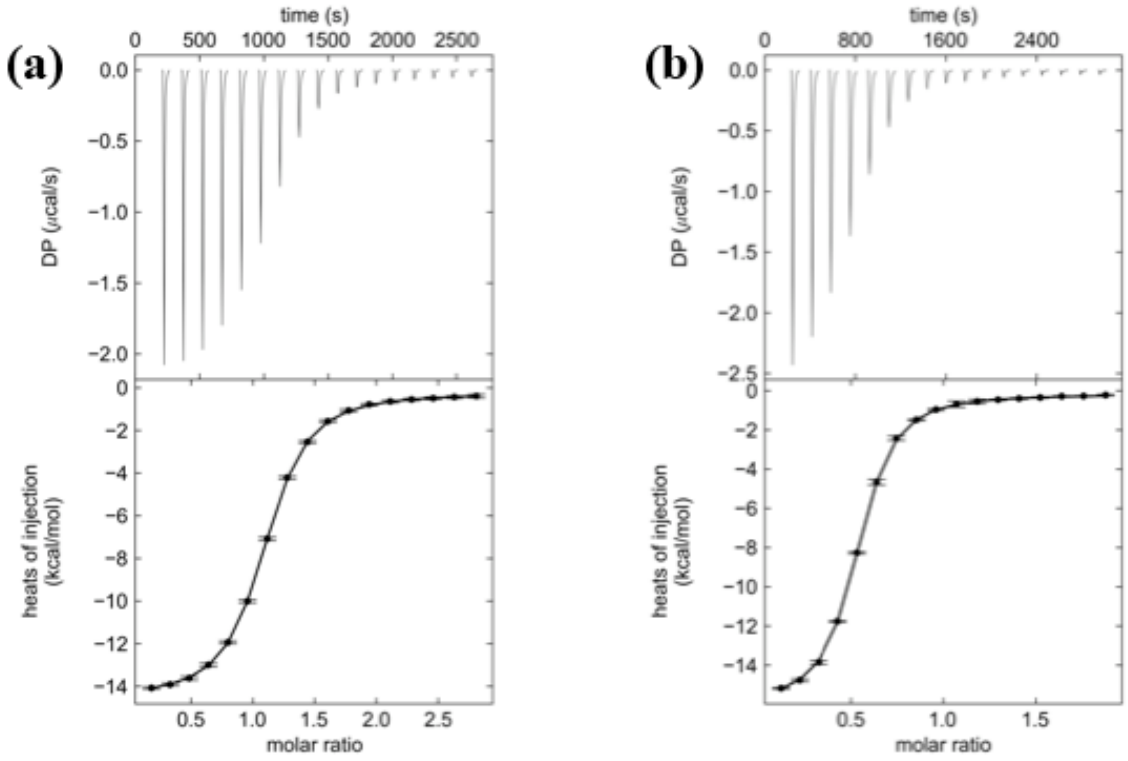

Fig. S7. ITC thermograms of (a) SH3 and (b) UIM-SH3 binding to the catalytic domain of AMSH revealing K_Ds of 1.4 ± 0.04 and 1.9 ± 0.1 μM, respectively.

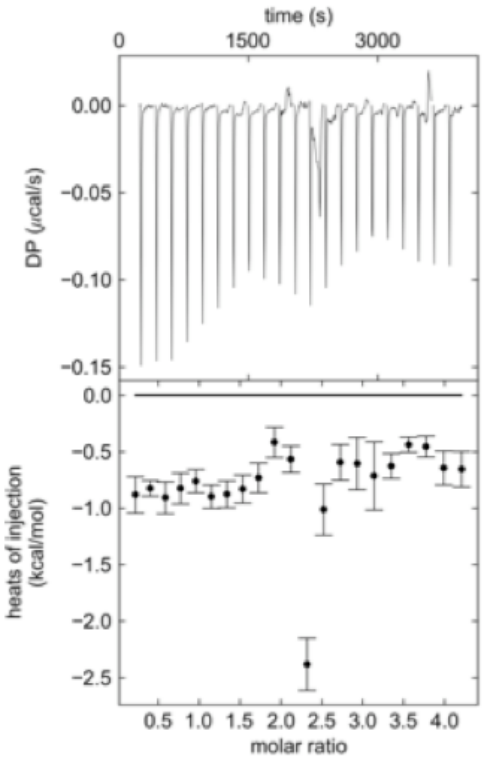

Fig. S8. Representative ITC thermogram of the titration of UIM-SH3 into the Lys238Thr mutant of the catalytic domain of AMSH showing no binding.

Supplementary Table 3. AMSH Activation Data

Protein	k_{cat} **(s^{-1})**	K_M **(μM)**
AMSH	1.4 ± 0.1	32 ± 5
AMSH + UIM-SH3	5 ± 1	19 ± 3